[8]Smart, M. K., Kalkhoran, I. M., and Bentson, J., "Measurements of Supersonic Wing Tip Vortices," *AIAA Journal*, Vol. 33, No. 10, 1995, pp. 1761–1768.

M. Sichel
Associate Editor

Vortex Shedding and Spacing of a Rotationally Oscillating Cylinder

T. Lee,* D. Birch,† and P. Gerontakos†
McGill University, Montreal, Quebec H3A 2K6, Canada

Introduction

THE possibility of the suppression or elimination of vortex shedding is of considerable practical interest from the standpoint of wake modification and reduction of drag, as well as of flow-induced vibration. Various passive and active control schemes have been attempted to affect the vortex wake formation process. Recently, it has been shown that a considerable amount of control of the cylinder vortex wake can be achieved through rotational oscillation and that when the flow takes place in a fluid relative to a rotationally oscillating cylinder, a new series of flow phenomena could arise.[1–4]

Tenada[1] studied the effects of rotational oscillation for $Re(=du_\infty/\nu$, where ν is the fluid viscosity) ranging between 30 and 300, and indicated that, at very high oscillation frequency f_0 and amplitude, the dead-fluid region behind a cylinder and the vortex-shedding process could be nearly eliminated. The amplitude is given by $\Omega_1 = \pi\Delta\theta f_0 d/2u_\infty > 7$–$27$, where $\Delta\theta$ is the peak-to-peak amplitude in degrees, d is the cylinder diameter, and u_∞ is the freestream velocity. Recently, Filler et al.[2] studied experimentally the frequency response of the shear layers separating from a circular cylinder subjected to small-amplitude oscillations, that is, $\Omega_1 \leq 0.03$, for $Re = 250$–1200, and observed a coupling of the cylinder oscillations with both modes of vortex shedding, that is, shear-layer vortices and primary Kármán vortex shedding. Filler et al. also reported that by rotationally oscillating the cylinder at or near the natural Kármán frequency, the shear-layer instability was promoted and the Kármán mode of vortex shedding was also affected. On the other hand, Tokumaru and Dimotakis[3] have shown that large-amplitude ($\Omega_1 \leq 16$) and high-frequency ($f_0/f_k = 1$–20, where f_k is the natural Karman shedding frequency) rotational oscillations, together with the spinning of the cylinder, can suppress the vortex shedding and produce significant reduction in the profile drag acting on the cylinder at $Re = 1.5 \times 10^4$.

The objective of this study was to investigate the variation of the lateral and longitudinal spacings of the shed vortices and the vortex formation with the cylinder oscillation at $Re = 1.75 \times 10^3$ by the use of hydrogen-bubble and particle streakline flow visualization methods. Special attention was given to the study of the type of wake synchronization that might occur throughout an intermediate oscillation range ($f_0/f_k < 4$ and $\Omega_1 \leq 1.0$), between those of Filler et al. and Tokumaru and Dimotakis.

Received 24 December 2002; revision received 27 October 2003; accepted for publication 14 January 2004.

*Associate Professor, Department of Mechanical Engineering. Member AIAA.

†Graduate Research Assistant, Department of Mechanical Engineering.

Experimental Methods

The experiment was conducted in a $45 \times 45 \times 180$ cm water towing tank. A polished hollow aluminum circular cylinder with a diameter of 2.54 cm and a length of 40 cm, fitted with an endplate, mounted vertically in the center of the tow carriage, was used as the test model. The origin of the coordinates was taken at the center of the cylinder with the x and y axes measured in the streamwise and transverse directions, respectively. The cylinder was rotated sinusoidally with $\Omega(t) = \Omega_1 \sin 2\pi f_0 t$ by a stepper motor. The cylinder rotary motion was monitored with a TRW type DP801 potentiometer (with an accuracy of ± 0.1 deg). A dc servomotor with a towing speed varying from 4 to 12 cm/s was used to drive the towing carriage. The initial acceleration and final deceleration of the towing speeds were carefully programmed to minimize the flow disturbance or nonuniformity induced by the impulsive motion of the cylinder and their effects on the vortex formation. The frequency of the vortex wake and the uniformity of the flow were also measured directly by the use of a cylindrical hot-film probe (TSI Model 1210-20W) incorporating an HP 3584A full Fourier transform (FFT) spectrum analyzer and an oscilloscope, respectively. Long-exposure particle streaklines and hydrogen-bubble flow visualizations were also recorded on Kodak T-MAX 400 film with a 35-mm Nikon camera and a 30-Hz video camera, respectively. The video film was studied frame-by-frame to determine the changes in the pattern and spacing of the shed vortices.

Results and Discussion

Figs. 1b–1i show the vortex streets for $f_0 < 4f_k$ at $\Omega_1 = 1.0$ with $Re = 1.75 \times 10^3$. Depending on the values of oscillation frequency and amplitude, three fundamental types of vortex lock-on were observed. At $f_0 = \frac{1}{2} f_k$, a subharmonic form of lock-on took place whereby the vortex shedding approached a single line of vortices of alternate signs with a significantly increased longitudinal, l, spacing and a vanishing lateral, h, spacing of the vortex street, that is, near the limit of vortex spacing ratio $h/l = 0$, Fig. 1b, compared to that of a stationary cylinder (Fig. 1a). In contrast, at oscillation frequencies near or at the Kármán frequency ($f_0 = 0.75$–$1.25 f_k$), the lock-on took place as vortices were shed alternately from the cylinder to form an altered vortex street (Figs. 1c–1e), similar to the classical Kármán vortex street but with different values of h and l. The lock-on phenomena were found to be similar to the results of Griffin and Ramberg[5] for a cylinder vibrating laterally with the vortex and vibration frequency synchronized. Figures 1f–1i show that for a cylinder oscillated at a multiple of the Kármán frequency ($f_0 = 1.5$–$4 f_k$), the vortex street took on an appearance of largely parallel vortex shedding mode, specifically, a contracted alternating vortex pattern like a normal vortex street but with vortex centers parallel to the wake centerline, resembling jetlike flows. No discernible vortex formation region and shear-layer instability were observed in the present experiment, as opposed to the observed coupling of the small-amplitude cylinder oscillation with both secondary and primary vortices of Filler et al. For the present range of oscillation conditions investigated, the separated shear layers were highly disturbed and with sufficient vorticity, thus allowing a growing vortex behind the oscillating cylinder to roll up quickly, eliminating or suppressing the necessity of drawing the opposite shear layer across the wake (as opposed to the natural vortex formation process existing behind a stationary cylinder, as proposed by Gerrard[6]). Also, an oscillation amplitude as low as $\Omega_1 = 0.25$, instead of a minimum value of Ω_1 of 2 as recommended by Tokumaru and Dimotakis,[3] was needed to send the vorticity stored in the boundary layer into the wake in a regular manner.

Figures 1j–1n also show that, depending on the values of f_0 and Ω_1, the wake unlocked from the oscillation of the cylinder and rendered dramatic change in the vortex shedding modes. The conceptual diagrams of the periodic and synchronized vortex patterns are shown in Fig. 2. Similar to the work of Williamson and Roshko,[7] who studied the synchronized wake behind a cylinder subjected to a sinusoidal trajectory in an X–Y towing tank, the lock-on vortex streets shown in Figs. 1c–1i can be represented by the $2S$ vortex mode, which indicates that in each one-half cycle a vortex was

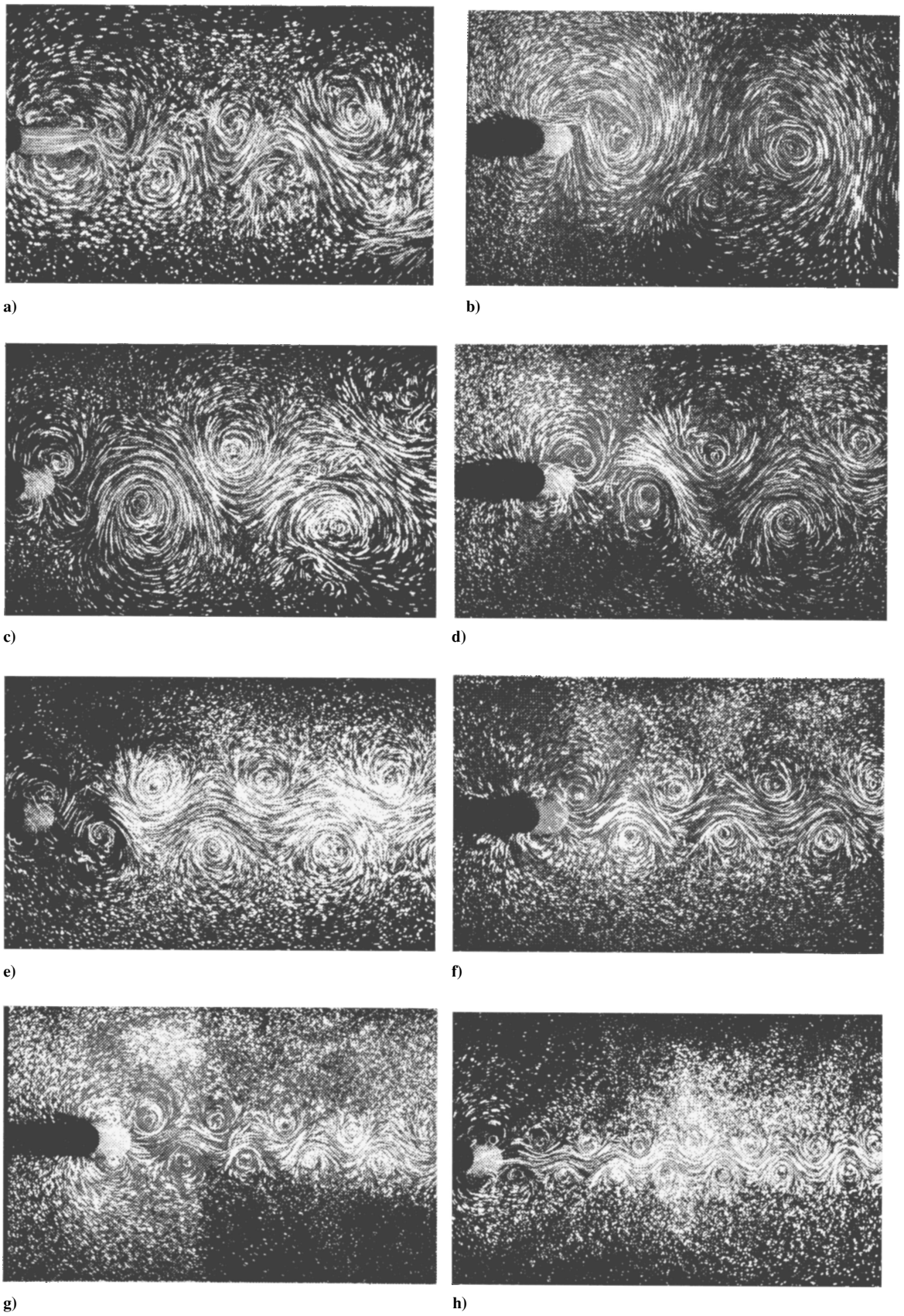

Fig. 1 Vortex patterns at $Re = 1.75 \times 10^3$: a) stationary cylinder; oscillating cylinder with $\Omega_1 = 1$: b) $f_0/f_k = 0.5$, c) $f_0/f_k = 0.75$, d) $f_0/f_k = 1$, e) $f_0/f_k = 1.25$, f) $f_0/f_k = 1.5$, g) $f_0/f_k = 2$, h) $f_0/f_k = 2.5$, and i) $f_0/f_k = 3$; $\Omega_1 = 0.25$: j) $f_0/f_k = 2$ and k) $f_0/f_k = 2.5$; l) $\Omega_1 = 0.25$ and $f_0/f_k = 0.5$; $\Omega_1 = 0.5$: m) $f_0/f_k = 2$ and n) $f_0/f_k = 3$ (flow from left to right, photographs taken at the end of counterclockwise (CCW) rotation of the cylinder.

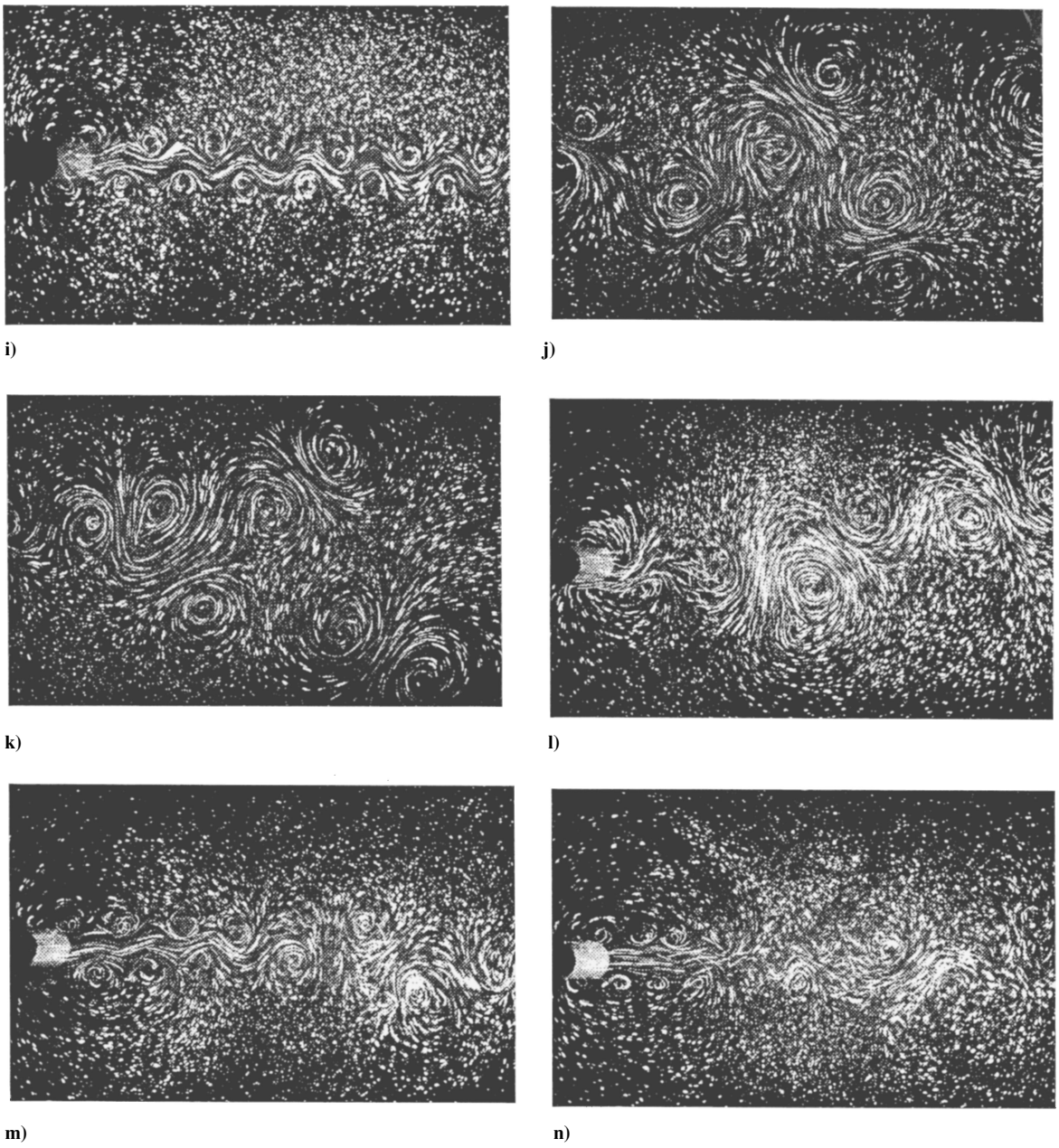

Fig. 1 Vortex patterns at $Re = 1.75 \times 10^3$: a) stationary cylinder; oscillating cylinder with $\Omega_1 = 1$: b) $f_0/f_k = 0.5$, c) $f_0/f_k = 0.75$, d) $f_0/f_k = 1$, e) $f_0/f_k = 1.25$, f) $f_0/f_k = 1.5$, g) $f_0/f_k = 2$, h) $f_0/f_k = 2.5$, and i) $f_0/f_k = 3$; $\Omega_1 = 0.25$: j) $f_0/f_k = 2$ and k) $f_0/f_k = 2.5$; l) $\Omega_1 = 0.25$ and $f_0/f_k = 0.5$; $\Omega_1 = 0.5$: m) $f_0/f_k = 2$ and n) $f_0/f_k = 3$ (flow from left to right, photographs taken at the end of CCW rotation of the cylinder (continued).

shed into the downstream distance, like the natural Kármán vortex shedding but with varied vortex spacings. The dashed lines in Fig. 2 enclosed those vortices formed in one complete cycle. Figure 1j shows that for $\Omega_1 = 0.25$ with $f_0 = 2f_k$, the vortex patterns were dramatically different from the $2S$ mode and were characterized by two vortex pairs shed during each oscillation cycle, that is, $2P$ mode. With a further increase in the oscillation frequency ($f_0 = 2.5f_k$), a combination of $P + S$ mode was observed (Fig. 1k), or a vortex pattern wherein each cycle a vortex pair and a single vortex were shed. The $P + S$ mode evolved into a $2P + 2S$ mode when the oscillation frequency was reduced to one-quarter of the natural Kármán frequency ($f_0 = \frac{1}{4} f_k$) with $\Omega_1 = 0.5$, a peculiar vortex wake wherein each one-half cycle a vortex pair and a single vortex were shed (Fig. 1l). Because of the insufficient level of resolution of the near wake structure, the causes for the observed changes in the intermediate wake could not be determined clearly. The analysis of the hydrogen-bubble results of the dynamics of the forming vortices at the cylinder surface during counterclockwise and clockwise oscillation of the cylinder, however, showed great similarity to the results of Williamson and Roshko.[7] Detailed explanations of the mechanisms responsible for the observed changes in the $2P$, $P + S$, and $2P + 2S$ vortex shedding modes and the accompanying widening and narrowing of the wake are given by these investigators.

Figures 1m and 1n further indicate that the vortex streets, in addition to the periodic and synchronized vortex patterns that prevailed for 18 diameters downstream distance as observed in Figs. 1a–1l, can also coalesce into a large-scale streetlike wake structure with lower spatial frequency after a few cylinder diameters downstream. Figure 1m shows that the parallel $2S$ mode persisted in the near wake (covering about $7d$ downstream distance) and was followed by single vortex pairing (P mode) for $f_0/f_k = 2$ at $\Omega_1 = 0.5$. The coalescence of the small-scale $2S$ mode vortex wake and the vigorous interaction of the viscous cores of the vortices $5d$ downstream of the cylinder can be more clearly seen for $f_0/f_k = 3$ (Fig. 1n); the flow along the centerline of the wake became highly irregular and broke down to turbulence. The mechanisms responsible for the observed phenomena, however, are not clear.

Figure 3 summarizes the variation of the lateral and longitudinal spacing of the shed vortices with f_0 at $\Omega_1 = 1.0$. These measurements were obtained directly from an average of 15 images with a

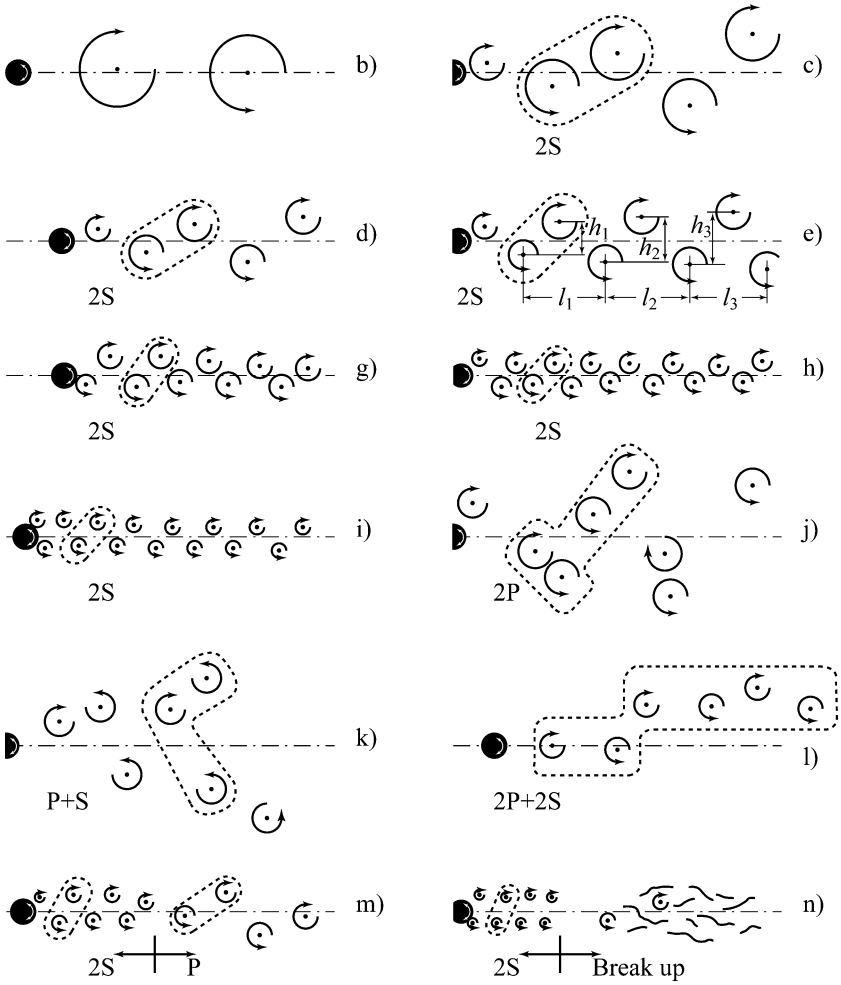

Fig. 2 Vortex patterns shown in Fig. 1.

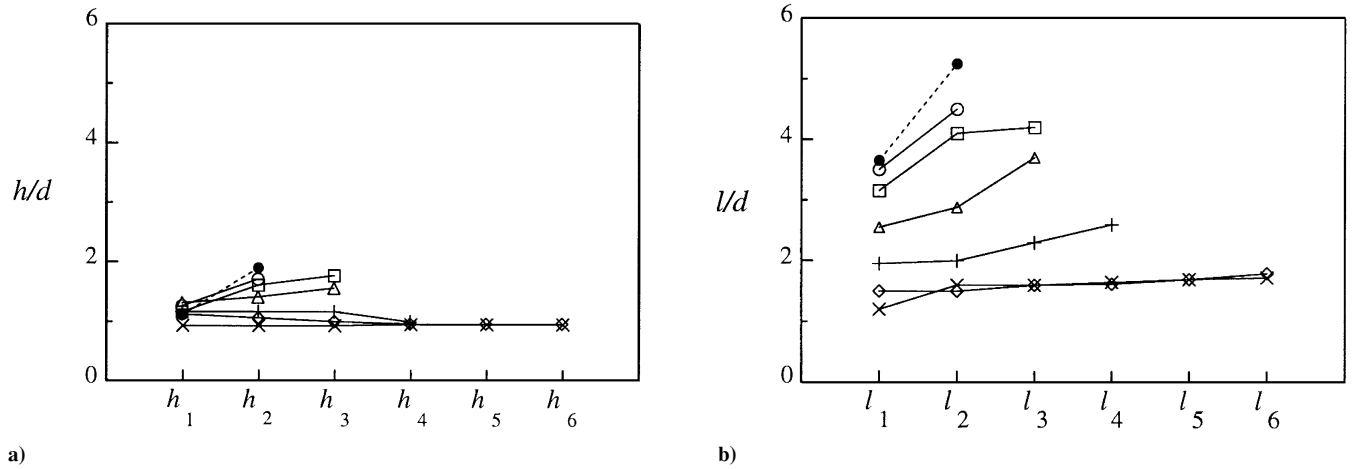

Fig. 3 Variation of a) lateral, h/d and b) longitudinal, l/d, spacings at $\Omega_1 = 1$: ○, $f_0/f_k = 1$; □, $f_0/f_k = 1.25$; △, $f_0/f_k = 1.5$; +, $f_0/f_k = 2$; ◇, $f_0/f_k = 2.5$; and ×, $f_0/f_k = 3$; ●, stationary cylinder (definition of h_1 and l_1 given in Fig. 2e).

discrepancy within ±3%. The lateral spacing of the shed vortices decreased to a value smaller than that of a stationary cylinder with increasing frequency (Fig. 3a) and became insensitive to the change in the oscillation frequency for $f_0 > 2f_k$. Similar to the change of lateral spacing with the oscillation frequency, the longitudinal spacing was found to decrease, but at a much greater degree, with increasing oscillation frequency (Fig. 3b). The longitudinal spacing was found to be not quite as dependent on the oscillation amplitude. The value of the h/l spacing ratio was found to increase with oscillation frequency, and this behavior appeared to be principally caused by the strong inverse dependence of the longitudinal vortex on the forcing frequency. For $f_0 > 1.25f_k$, the value of h/l ratio, corresponding to the $2S$ lock-on mode indicated in Figs. 1f–1i, became greater than that of a stationary cylinder.

Conclusions

The vortex wake behind a rotationally oscillating circular cylinder at $Re = 1.75 \times 10^3$ was investigated. Depending on the forcing frequency and amplitude, different vortex-shedding modes, similar to those observed for a cylinder in transverse[6] and sinusoidal

motion,[7] were observed. The vortex wake expanded for oscillation frequencies less than the Kármán frequency, whereas it contracted for frequencies greater than the Kármán frequency. The longitudinal spacing decreased significantly with increasing oscillation frequency and changed to a much lesser degree with an increase in the oscillation amplitude. In contrast, the lateral spacing of the shed vortices showed a relatively weaker dependence on the rotary oscillation. Further experiments on the vortex strength and formation are needed to better understand the characteristics of the various synchronized wake patterns.

References

[1]Tenada, S., "Visual Observations of the Flow past a Circular Cylinder Performing a Rotary Oscillation," *Journal of Physics Society of Japan*, Vol. 45, 1978, pp. 1038–1043.

[2]Filler, J. R., Marston, P. L., and Mih, W. C., "Response of the Shear Layers Separating from a Circular Cylinder to Small-Amplitude Rotational Oscillation," *Journal of Fluid Mechanics*, Vol. 231, 1991, pp. 481–499.

[3]Tokumaru, P. T., and Dimotakis, P. E., "Rotary Oscillation Control of a Cylinder Wake," *Journal of Fluid Mechanics*, Vol. 224, 1991, pp. 77–90.

[4]Fujisawa, N., Kawaji, Y., and Ikemoto, K., "Feedback Control of Vortex Shedding from a Circular Cylinder by Rotational Oscillations," *Journal of Fluids and Structures*, Vol. 15, 2001, pp. 23–37.

[5]Griffin, O. M., and Ramberg, S. E., "The Vortex-Street Wakes of Vibrating Cylinders," *Journal of Fluid Mechanics*, Vol. 66, 1974, pp. 553–576.

[6]Gerrard, J. H., "The Mechanisms of the Formation Region of Vortices Behind Bluff Bodies," *Journal of Fluid Mechanics*, Vol. 25, 1966, pp. 401–413.

[7]Williamson, C. H. K., and Roshko, A., "Vortex Formation in the Wake of an Oscillation Cylinder," *Journal of Fluids and Structures*, Vol. 2, 1988, pp. 355–381.

W. J. A. Dahm
Associate Editor

Pre-Limit-Point Buckling of Multilayer Cylindrical Panels Under Pressure

S. E. Rutgerson* and W. J. Bottega†
Rutgers University, Piscataway, New Jersey 08854-8058

I. Introduction

THIN shell structures, whether isotropic or composite, are seen in a wide variety of applications. In many situations the primary consideration is that of buckling of shell structures, particularly because of distributed (pressure) loads and point loads. An interesting, and perhaps common, phenomenon seen experimentally[1] is the onset of snap-through well below the limit load for force controlled tests. Pre-limit-point behavior is discussed analytically by Thompson and Hunt,[2] Simitses,[3] and by Pi and Trahair[4] for isotropic structures, but is often overlooked in many analyses. More recently, pre-limit-point buckling was identified for thermally loaded multilayer shell segments by Rutgerson and Bottega.[5]

In the present Note, buckling behavior of multilayer shallow shell segments subjected to external pressure is considered for plane-strain (long panel)/plain-stress (shallow arch) configurations with either clamped-fixed or pinned-fixed support conditions. The mathematical model, mixed formulation, and solution techniques presented and employed in Ref. 5 are applied to the present problem. It is shown that critical behavior, in the form of pre-limit-point snap-through buckling, is a function of a length ratio and a stiffness ratio of the composite structure. It is seen from numerical simulations that when snap-through buckling occurs it occurs below the limit load, often at values well below those that would be predicted from the limit point and that such behavior is pervasive.

II. Problem Statement

Consider the multilayer shell shown in Fig. 1. The structure will be considered to be composed of n layers, with the innermost layer of the composite shell denoted as layer 1 and the outermost layer as layer n. A convenient surface, say the interface between two layers or the geometric center of the structure, is used as the reference surface, and all length scales are normalized with respect to the dimensional radius of the undeformed reference surface. In doing so, the structure is described by the angular coordinate θ measured from the center of the span, and the half-length of the structure is defined by the angle ϕ^*. The structure is thus defined over the domain $-\phi^* \le \theta \le \phi^*$. A shallow shell theory is used as the mathematical model for each layer.[5]

The problem is stated in a mixed formulation in terms of the (normalized) radial displacement $w(\theta)$ (positive toward center of curvature) and the (normalized) resultant membrane force $\hat{N}$ (positive in compression). The equations and boundary conditions of Ref. 5 are applied to the present problem and are presented here. Hence,

$$w'''' + (2 + \hat{N})w'' + w = \hat{p} - (1 - \rho^*)\hat{N}, \qquad \theta \in [0, \phi^*] \tag{1a}$$

$$\hat{N}' = 0, \qquad \theta \in [0, \phi^*] \tag{1b}$$

$$w'(0) = 0 \tag{2a}$$

$$[w''' + (1 + \hat{N})w']_{\theta=0} = 0 \tag{2b}$$

$$w(\phi^*) = 0 \tag{2c}$$

$$w'(\phi^*) = 0 \tag{2d$_1$}$$

or

$$[w'' + w]_{\theta=\phi^*} = 0 \tag{2d$_2$}$$

where a superposed prime indicates total differentiation with respect to θ. Further, $\hat{p}$ is the nondimensional pressure and $\hat{N}$ is

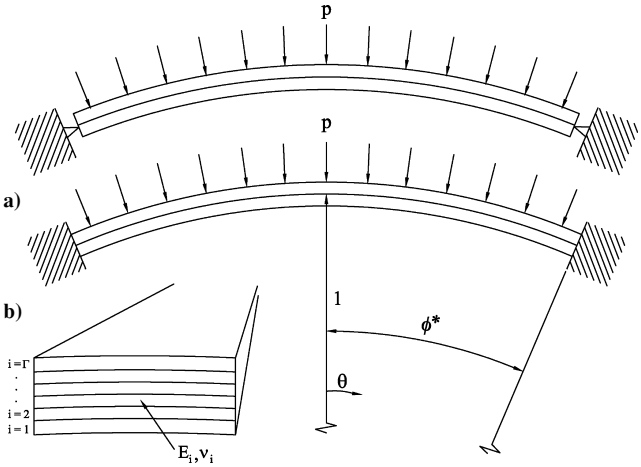

Fig. 1 Multilayer shell: a) pinned-fixed supports and b) clamped-fixed supports.

Received 17 January 2002; revision received 12 August 2003; accepted for publication 5 February 2004.

*Graduate Student; currently Structural Engineer, Naval Surface Warfare Center, Carderock Division, West Bethesda, MD 20817-5700.

†Associate Professor, Department of Mechanical and Aerospace Engineering. Associate Fellow AIAA.